

# Analytical Methods

Accepted Manuscript



This is an *Accepted Manuscript*, which has been through the Royal Society of Chemistry peer review process and has been accepted for publication.

*Accepted Manuscripts* are published online shortly after acceptance, before technical editing, formatting and proof reading. Using this free service, authors can make their results available to the community, in citable form, before we publish the edited article. We will replace this *Accepted Manuscript* with the edited and formatted *Advance Article* as soon as it is available.

You can find more information about *Accepted Manuscripts* in the [Information for Authors](#).

Please note that technical editing may introduce minor changes to the text and/or graphics, which may alter content. The journal's standard [Terms & Conditions](#) and the [Ethical guidelines](#) still apply. In no event shall the Royal Society of Chemistry be held responsible for any errors or omissions in this *Accepted Manuscript* or any consequences arising from the use of any information it contains.

1  
2  
3  
4 1 **Colorimetric determination of ammonium persulfate in**  
5  
6 2 **water-borne adhesive for cigarette based on silver triangular**  
7  
8 3 **nanoparticles**

9  
10  
11 4 Yanqun Xu<sup>a</sup>, Anyi Chen<sup>b</sup>, Ruizhi Zhu<sup>a</sup>, Naiding Wang<sup>a</sup>, Zhigang Tai<sup>b</sup>, Hongtao  
12  
13 5 Feng<sup>a\*</sup>

14  
15  
16 6 **Abstract**

17  
18  
19 7 In this paper, a simple method for the determination of ammonium persulfate  
20  
21 8 using silver triangular nanoparticles (silver TNPs) was developed. Specifically, silver  
22  
23 9 TNPs exhibited strong appreciable surface plasmon resonance (SPR) signals at 670  
24  
25 10 nm, and low concentration of ammonium persulfate could induce an SPR decrease of  
26  
27 11 silver TNPs with color changed from blue to colorless. Furthermore, it was also found  
28  
29 12 that the SPR decreasing intensity was proportional to the concentration of ammonium  
30  
31 13 persulfate over the range of 0.10-0.70 mmol L<sup>-1</sup>, with a correlation coefficient of  
32  
33 14 0.9994. The spiked recoveries were in the range of 94.4%-105.8% with RSD of  
34  
35 15 3.3%-5.6%. Finally, a method for ammonium persulfate detection by UV-vis  
36  
37 16 spectrophotometric was established and successfully applied for determination of  
38  
39 17 ammonium persulfate in water-borne adhesive for cigarette.  
40  
41  
42  
43  
44  
45  
46  
47  
48

49 19 **Key words:** silver triangular nanoparticles, ammonium persulfate, colorimetric  
50  
51  
52  
53  
54  
55  
56  
57  
58  
59  
60

## 20 1. Introduction

21 It is well known that the quality of cigarette materials is one of the key factors  
22 affecting the quality and grade of cigarette products. Water-borne adhesive, as one  
23 kind of cigarette materials, is frequently used for gluing of cigarette lap and cigarette  
24 filter. However, some chemicals which do harm to respiratory system and immune  
25 system would be introduced into water-borne adhesive in the process of manufacture  
26 for technical reason.<sup>1,2</sup> Therefore, the detection methodology of harmful chemicals in  
27 water-borne adhesive had been widely studied.

28 Ammonium persulfate was often used as an initiator in the synthesis of water-borne  
29 adhesive due to its strong oxidation performance.<sup>3</sup> And there always have some  
30 residual ammonium persulfate in water-borne adhesive used for cigarette  
31 manufacturing, which may either cause or intensify diseases such as asthma and skin  
32 reactions to smoker.<sup>4,5</sup> Therefore, it is necessary to set up analysis methods to monitor  
33 ammonium persulfate in water-borne adhesive, since ammonium persulfate is an ionic  
34 compound, the determination of ammonium persulfate is equal to the determination of  
35 persulfate in water-borne adhesive. As we all known that, persulfate with strong  
36 oxidant has been widely used for water and soil decontaminants,<sup>6</sup> circuit board  
37 fabrication,<sup>7</sup> cosmetics,<sup>8</sup> and polymerization,<sup>9</sup> and a number of methods have been  
38 reported for the determination of persulfate, such as reductometric,<sup>10, 11</sup>  
39 spectrophotometric,<sup>12, 13</sup> and electrochemical methods.<sup>14,15</sup> Most of these reported  
40 methods were excellent performance, but suffer from some drawbacks such as  
41 time-consuming and labor intensive.

1  
2  
3  
4 42 In recent years, silver nanoparticles (Ag NPs) have attracted great interests as a  
5  
6 43 colorimetric probe, which can directly detect analytes by monitoring the color change  
7  
8  
9 44 using UV-vis spectroscopy or even with naked eyes. Apparently, nearly no  
10  
11 45 complicated instruments are involved in the detection procedures. Furthermore, the  
12  
13 46 color change is highly sensitive to the size, shape, capping agent, medium refractive  
14  
15  
16 47 index, and state of Ag NPs. Many successful examples have been reported in the  
17  
18 48 determination of analytes regarding to environmental contaminations,<sup>16-18</sup> food  
19  
20 49 safety,<sup>19</sup> pharmaceutical analysis.<sup>20</sup> Silver triangular nanoparticles (silver TNPs) as  
21  
22  
23 50 one kind of anisotropic Ag NPs has been extensively investigated, since the  
24  
25  
26 51 extraordinarily plasmonic features across visible-NIR regions. Silver TNPs exhibit  
27  
28 52 intense and tunable localized surface plasmon resonance (SPR) and have been utilized  
29  
30  
31 53 to analytical chemistry with satisfactory results.<sup>21-26</sup>

32  
33  
34 54 In this paper, it was found that the ammonium persulfate could oxidize the silver  
35  
36 55 TNPs and decrease the SPR band of silver TNPs. Low concentration of ammonium  
37  
38  
39 56 persulfate had a good affinity to silver TNPs, and resulting in a transformation of Ag<sup>0</sup>  
40  
41 57 to Ag<sup>+</sup> with solution color changing from blue to colorless. The color of silver NPs  
42  
43  
44 58 changes with the decrease of SPR band of silver TNPs, a linear relationship was  
45  
46  
47 59 obtained between the concentration of ammonium persulfate and the maximum  
48  
49 60 absorbance of silver TNPs. Thus, a simple analytical method was developed to detect  
50  
51  
52 61 ammonium persulfate by using silver TNPs.

## 62 **2. Experimental**

### 63 **2.1. Materials**

1  
2  
3  
4 64 All commercially available reagents were of analytical grade. Silver nitrate ( $\text{AgNO}_3$ ,  
5  
6 65 99.8%) was purchased from Dingguochangsheng Biological Technology Co., Ltd.  
7  
8  
9 66 (Beijing, China). Trisodium citrate dehydrate ( $\text{C}_6\text{H}_5\text{O}_7\text{Na}_3 \cdot 2\text{H}_2\text{O}$ , 99.0%) was  
10  
11 67 purchased from Tianjin Chemical Reagent Co., Ltd. Sodium borohydride ( $\text{NaBH}_4$ ,  
12  
13 68 96.0%) was bought from Sinopharm Chemical Reagent Co., Ltd. (Shanghai, China).  
14  
15  
16 69 Hydrogen peroxide ( $\text{H}_2\text{O}_2$ , 30wt. %) was purchased from Chuangdong Chemical Co.,  
17  
18  
19 70 Ltd. (Chongqing, China). Ammonium persulfate ( $(\text{NH}_4)_2\text{S}_2\text{O}_8$ , 98.0%) was bought  
20  
21 71 from Guanghua Chemical Reagent Co., Ltd. (Guangdong, China). The pH value of  
22  
23 72 the reaction systems were controlled by Britton-Robinson (B-R) buffer solutions.  
24  
25  
26 73 Three batches of water-based adhesive for tobacco came from China Tobacco Yunnan  
27  
28  
29 74 Industrial Co. Ltd.

## 30 31 75 **2.2. Instruments**

32  
33  
34 76 Transmission electron microscope (TEM) patterns were conducted under JEM 2100  
35  
36 77 and operated at 200 kv. The specimen was prepared by dropping the solution onto the  
37  
38  
39 78 copper grids and air dried naturally. UV-vis absorption spectrum was obtained on a  
40  
41 79 UV-2550 spectrophotometer (Shimadzu, Japan) equipped with a 1-cm quartz cell.  
42  
43  
44 80 Atomic absorption spectrometry (AAS) was obtained using a Z-2000 polarized  
45  
46 81 Zeeman atomic absorption spectrophotometer (Hitachi, Japan). The pH value of the  
47  
48  
49 82 solution was measured by a pH meter (Lei Ci Instrument Factory, Shanghai, China). A  
50  
51 83 sczl-2 magnetic stirrer (Yu Hua Instrument Inc. Gongyi, China) was used to blend the  
52  
53  
54 84 solutions in a round-bottom flask to prepare the silver TNPs. An H-1850 centrifuge  
55  
56 85 was used in pretreatment of samples (Xiang Yi Instrument Inc. Hunan, China). A  
57  
58  
59  
60

1  
2  
3  
4 86 SB-2000 water bath pot (Shanghai Instrument Inc. Shanghai, China) was employed to  
5  
6 87 heat the silver colloids in the aging process.  
7

### 88 **2.3. Preparation of silver TNPs**

89 Silver TNPs were synthesized following the procedure conducted by Mirikin et al  
90 with some modification.<sup>27-30</sup> Typically, 24.75 mL of deionized water were added to a  
91 50 mL round-bottom flask and continuously magnetically stirred at room temperature  
92 in the presence of air. Subsequently, silver nitrate ( $0.1 \text{ mmol L}^{-1}$ , 25  $\mu\text{L}$ ), trisodium  
93 citrate ( $75 \text{ mmol L}^{-1}$ , 500  $\mu\text{L}$ ), hydrogen peroxide (30 wt.%, 60  $\mu\text{L}$ ) were successively  
94 added to the deionized water. Next, sodium borohydride ( $100 \text{ mmol L}^{-1}$ , 100  $\mu\text{L}$ ) was  
95 rapidly injected into the above mixture. The color of colloid turned to pale yellow  
96 immediately, suggesting the reduction of silver. After 1-2 min, the colloid changed to  
97 deep-yellow, indicating the formation of small silver nanoparticles. Over the next  
98 several minutes, the color of the colloid continued to change from yellow to red.  
99 Depending on the different amount of  $\text{NaBH}_4$  used, the final color of the solution  
100 ranged from red (35  $\mu\text{L NaBH}_4$ ) to blue (100  $\mu\text{L NaBH}_4$ ), as shown in Figure S1. The  
101 formation of silver TNPs was confirmed by TEM characterization, the morphology  
102 had clearly triangular corners. As shown in Figure 1, the UV-vis absorption peak  
103 wavelength of silver TNPs was about 670 nm.

104 The concentration of the silver TNPs solution was defined by its UV-vis absorption  
105 using the Beer-Lambert Law ( $c = A/\epsilon \cdot b$ ), where A is the maximum absorbance of  
106 silver TNPs at the maximum wavelength,  $\epsilon$  is the molar extinction coefficient of silver  
107 TNPs, b is the optical length which is usually 1.0 cm. However, the molar extinction

1  
2  
3  
4 108 ( $\epsilon$ ) of silver TNPs is uncertain in each preparation. Therefore, we use “X” as the value  
5  
6 109 of  $1/\epsilon$ , and thus,  $A \cdot X$  as the concentration of silver TNPs  
7  
8

#### 9 110 **2.4. General procedures**

10  
11 111 The detection of ammonium persulfate were carried out by the following  
12  
13 112 procedures. First, 800  $\mu\text{L}$  of silver TNPs was added into a clear centrifugal tube (5.0  
14  
15 113 mL) with variable concentration of  $(\text{NH}_4)_2\text{S}_2\text{O}_8$ . Then, the mixture solution was  
16  
17 114 diluted by deionized water to a volume of 4.0 mL and heated in a water bath at 80 °C  
18  
19 115 for 30 min. The blank tests were carried out under the same conditions. Subsequently,  
20  
21 116 the resulting mixture was used for UV-vis spectral analysis. For sample detection,  
22  
23 117 0.5000 g of water-based adhesive for tobacco was firstly dissolved in 25 mL  
24  
25 118 deionized water and extracted for 15 minutes on an oscillator. The extract solution  
26  
27 119 was centrifuged at 18500 rpm for 10 minutes, and the supernatant was diluted 1.5 fold  
28  
29 120 and used for spectrophotometric detection after reacted with silver TNPs.  
30  
31  
32  
33  
34  
35

### 36 121 **3. Results and discussion**

#### 37 122 **3.1. Features of silver TNPs after interacted with ammonium persulfate**

38  
39 123 TEM, UV-vis spectrophotometer and AAS were used to study the mechanism of  
40  
41 124 reaction between silver TNPs and ammonium persulfate. Compared the spectrum with  
42  
43 125 reported reference,<sup>27, 31-33</sup> the SPR absorption spectrum of silver TNPs prepared here  
44  
45 126 showed a weak transversal out-of-plane quadrupole band (334 nm), out-of-plane  
46  
47 127 dipole band (430 nm) and a very intense in-plane dipole band (670 nm) (shown as  
48  
49 128 Figure 1). After addition of ammonium persulfate in silver TNPs solution and heated  
50  
51  
52  
53  
54  
55 129 for 30 min at 80 °C, the color of silver TNPs suspension changed from blue to  
56  
57  
58  
59  
60

1  
2  
3  
4 130 colorless, the absorption peak of silver TNPs at 670 nm decreased with the increase of  
5  
6 131 ammonium persulfate concentration (Figure 2). TEM images of silver TNPs showed  
7  
8  
9 132 that the number of silver TNPs obviously reduced after ammonium persulfate was  
10  
11 133 added (Figure 3). This phenomenon suggested that the silver TNPs were oxidized by  
12  
13  
14 134 ammonium persulfate.

15  
16 135 To verify the silver ion production, the mixture of the  $(\text{NH}_4)_2\text{S}_2\text{O}_8$ -silver TNPs was  
17  
18 136 centrifuged at 18500 rpm for 10 minutes on the centrifuge, and the atomic absorption  
19  
20  
21 137 value of the top pellucid liquid was measured under the conditions of 328.1 nm, 2.0  
22  
23  
24 138 mA lamp current, 0.4 nm spectral pass band, air/acetylene flow rate of 15 L  $\text{min}^{-1}$ /2 L  
25  
26 139  $\text{min}^{-1}$ . The result showed that with the increase of  $(\text{NH}_4)_2\text{S}_2\text{O}_8$  concentration, the  
27  
28  
29 140 absorption value improved correspondingly (Table S1). The results demonstrated that  
30  
31 141 silver TNPs converted to silver ion after reacted with ammonium persulfate.

### 34 142 **3.2. The selection of analysis probe**

35  
36 143 Ag NPs used in this paper was prepared by conventional thermal route with slight  
37  
38 144 modification.<sup>29, 30</sup> Ag NPs with different colors were obtained by changing the amount  
39  
40  
41 145 of  $\text{NaBH}_4$  or  $\text{H}_2\text{O}_2$  during the preparation. As shown in Figure S1, the maximum  
42  
43  
44 146 absorption wavelength of Ag NPs was shifted with the color changed. Ag NPs with  
45  
46 147 different colors were studied for ammonium persulfate detection. After reacting with  
47  
48  
49 148 ammonium persulfate, a sequence of UV-vis spectrograms were obtained, the results  
50  
51  
52 149 showed that Ag NPs with different colors had the similar changing rule in the  
53  
54  
55 150 presence of ammonium persulfate (see supporting information, Figure S2, Figure S3,  
56  
57 151 Fig S4). The colorimetric method proposed by our group was based on comparing the  
58  
59  
60



1  
2  
3  
4 152 gradual spectrum changes in the presence of the analyte, and finding the relationship  
5  
6 153 between maximum absorbance and concentration of ammonium persulfate. The value  
7  
8  
9 154 of maximum absorbance can be used for describing the transformation process of  
10  
11 155 silver TNPs to  $\text{Ag}^+$ , with the concentration of  $(\text{NH}_4)_2\text{S}_2\text{O}_8$  increased, the value of  
12  
13 156 maximum absorbance decreased. Compared with red and purple silver colloid, blue  
14  
15  
16 157 silver colloid with higher value of maximum absorbance has wider linear range and  
17  
18  
19 158 higher sensitivity, thus the blue silver colloid was selected as the analysis probe.

### 20 21 159 **3.3. Effect of pH**

22  
23  
24 160 The pH of the test solution was one of the prime factors affecting the stability of  
25  
26 161 silver TNPs. Chen had found that the acidity affected the change of the shape and size  
27  
28 162 of silver TNPs.<sup>34</sup> Therefore, the pH influence on the system of silver  
29  
30 163 TNPs/ $(\text{NH}_4)_2\text{S}_2\text{O}_8$  was investigated. As Figure 4 showed that the value of maximum  
31  
32 164 absorbance of silver TNPs/ $(\text{NH}_4)_2\text{S}_2\text{O}_8$  system changed with the pH value. The value  
33  
34 165 of maximum absorbance achieved relative high and get stable in the range of  
35  
36 166 6.80-7.24. However, when the pH continues to increase, silver TNPs are unstable and  
37  
38 167 aggregate together (Supporting information, Figure. S5). Therefore, the pH 6.80 was  
39  
40 168 selected as optimum value.

### 41 42 169 **3.4. Effect of reaction temperature**

43  
44  
45  
46 170 The temperature of reaction was an important parameter, which has an influence on  
47  
48 171 reaction rate. The effect of reaction temperature on silver TNPs/ $(\text{NH}_4)_2\text{S}_2\text{O}_8$  system  
49  
50 172 has been investigated in the range of 20–90 °C using a water bath, and the result was  
51  
52 173 shown in Figure 5.  $\Delta$  (maximum absorbance) represented the extent of reaction  
53  
54  
55  
56  
57  
58  
59  
60

1  
2  
3  
4 174 between silver TNPs and  $(\text{NH}_4)_2\text{S}_2\text{O}_8$ , which was calculated as  $\Delta$  (maximum  
5  
6 175 absorbance) =  $A_{\text{max before}} - A_{\text{max after}}$ , where  $A_{\text{max before}}$  is the maximum absorbance of  
7  
8  
9 176 silver TNPs before reacted with  $(\text{NH}_4)_2\text{S}_2\text{O}_8$ , and  $A_{\text{max after}}$  is the maximum absorbance  
10  
11 177 of silver TNPs after reacted with  $(\text{NH}_4)_2\text{S}_2\text{O}_8$ . As can be seen, with the temperature  
12  
13 178 increased the value of  $\Delta$  (maximum absorbance) became smaller, indicating  
14  
15 179  $(\text{NH}_4)_2\text{S}_2\text{O}_8$  was reacted more and more completely. According to the control test,  
16  
17 180 silver TNPs became unstable at a high temperature (90 °C), which might lead to  
18  
19 181 erroneous results. Therefore, 80 °C was selected as optimum temperature of reaction  
20  
21 182 in the following experiments.

### 22 183 **3.5. Effect of reaction time**

23  
24  
25  
26 184 The effect of reaction time was carried out under the optimum conditions in the  
27  
28  
29 185 range of 10 to 60 min. Four different concentrations of ammonium persulfate were  
30  
31 186 used for the tests and the results were shown as Figure 6. With the reaction time  
32  
33 187 increased, the value of maximum absorbance of silver TNPs reacted with low  
34  
35 188 concentration of ammonium persulfate got stable quickly (within 20 min), while the  
36  
37 189 high concentration of ammonium persulfate would take a longer time. For accurate  
38  
39 190 determination of ammonium persulfate in real samples, 30 minutes was selected for  
40  
41 191 the optimum reaction time.

### 42 192 **3.6. Effects of coexistence substances**

43  
44  
45  
46 193 The effects of coexistence substances were carried under the optimum conditions, a  
47  
48  
49 194 number of substances which might exist in water-based adhesive and dissolve in water,  
50  
51 195 were investigated in this study (including formaldehyde, acetaldehyde, acetone,  
52  
53  
54  
55  
56  
57  
58  
59  
60

1  
2  
3  
4 196 butanal, crotonaldehyde, glyoxal, orthoboric acid, sodium bicarbonate,  $\text{Pb}^{2+}$ ,  $\text{As}^{3+}$ ,  
5  
6 197 ammonium persulfate). The results were shown as Figure 7, the higher concentration  
7  
8  
9 198 of coexistence substances did not affect the determination of ammonium persulfate,  
10  
11 199 which suggested this method had a good selectivity.

### 14 200 **3.7. Analytical performance**

16 201 The linearity of the method was tested under the optimum experimental conditions,  
17  
18 202 the calibration curve (Figure 8) was obtained with a good linearity in the range from  
19  
20 203 0.10 to 0.70  $\text{mmol L}^{-1}$ , and the regression coefficient ( $R^2$ ) was 0.9989. The detection  
21  
22 204 limit of ammonium persulfate in this sensing method was 0.01 mM ( $3\sigma$ ), which was  
23  
24 205 comparable to some reported persulfate assays. We compared this method with some  
25  
26 206 commonly used methods, the results (Table 1) indicated that the proposed method was  
27  
28  
29 207 a good platform for the detection of ammonium persulfate.

31  
32  
33 208 In order to study the validity of the proposed method, three batches of water-based  
34  
35 209 adhesive before and after spiking were used for the determination of ammonium  
36  
37 210 persulfate. The results were list in Table 1, As can be seen, the mean recoveries were  
38  
39 211 in the range from 94.4 to 105.8% at 0.2, 0.4, and 0.6  $\text{mmol L}^{-1}$  spiked levels, and the  
40  
41 212 relative standard deviations (RSDs) were in the range from 3.3% to 5.6%, the average  
42  
43 213 content of ammonium persulfate in the water-based adhesive for cigarette is 0.109  
44  
45 214  $\text{mmol L}^{-1}$  (1.84  $\text{mg g}^{-1}$ ). These parameters indicated that the present method with high  
46  
47 215 sensitivity and reliability could be used for the determination of ammonium persulfate  
48  
49 216 in water-based adhesive.

### 52 217 **3.8. Repeatability and reproducibility**

1  
2  
3  
4 218 Five batches of silver TNPs (with maximum absorption wavelength in range from  
5  
6 219 549 to 607 nm), which prepared at different days using same reagents, were used for  
7  
8  
9 220 ammonium persulfate detection. As shown in Table S2, the detection values were very  
10  
11 221 close to the defined concentrations. Thus, the colorimetric method proposed here have  
12  
13  
14 222 outstanding advantages of good precision and reproducibility.

#### 16 223 **4. Conclusions**

18  
19 224 In this contribution, a simple method for ammonium persulfate detection was  
20  
21 225 established according to the oxidation property of ammonium persulfate. The  
22  
23  
24 226 maximum absorbance of silver TNPs damped clearly with increasing the  
25  
26 227 concentrations of ammonium persulfate over the range of 0.10-0.70 mmol L<sup>-1</sup>. Good  
27  
28  
29 228 recoveries were obtained in the range of 94.4%-105.8% with RSD lower than 5.6%.  
30  
31 229 The proposed method for ammonium persulfate detection by UV-vis  
32  
33  
34 230 spectrophotometric observation has been applied to analysis of ammonium persulfate  
35  
36 231 in water based adhesive for cigarette with satisfactory results.

#### 38 232 **Acknowledge**

40  
41 233 This work was financially supported by the Starting Research Project of Importing  
42  
43  
44 234 Talented Teachers in Kunming University of Science and Technology  
45  
46 235 (KKSJ201226105) and the Analysis and Testing Foundation of Kunming University  
47  
48  
49 236 of Science and Technology (No. 20150653).

50  
51 237  
52  
53  
54  
55  
56  
57  
58  
59  
60

238 **Table 1. Comparison of analytical features for some reported persulfate assays**

Method	Probe	Linear range (mM)	Detection limit (mM)	Ref
Voltammetric	electrode modified with a Prussian blue film	0.05-3	Not given	35
Spectrophotometric	Methylene Blue	0-1.5	0.0028	36
Flow injection amperometric	Prussian Blue film-modified electrode	0.1-1.0	0.09	37
Colorimetric	Silver TNPs	0.1-0.7	0.01	This article

239

240

241

242 **Table 2.** Results for the determination of  $(\text{NH}_4)_2\text{S}_2\text{O}_8$  in water-based adhesive for  
243 cigarette

Sample No.	Added ( $\text{mmol L}^{-1}$ )	Found( $\text{mmol L}^{-1}$ )	Recovery(%)	RSD (%) (n=3)
	0	0.122		
1	0.2	0.304	94.4	5.6
	0.4	0.515	98.7	3.8
	0.6	0.719	96.7	5.1
	0	0.086		
2	0.2	0.291	105.8	3.7
	0.4	0.472	97.1	4.6
	0.6	0.663	96.6	3.8
	0	0.102		
3	0.2	0.297	98.3	3.5
	0.4	0.491	97.8	3.3
	0.6	0.688	98.0	4.8

244

245 **Notes and references**

246 <sup>a</sup> Research & Development Center, China Tobacco Yunnan Industrial Co., Ltd,  
247 Kunming, 650231, China. *Email:369546858@qq.com*

248 <sup>b</sup> Faculty of Science and Life Technology, Kunming University of Science and  
249 Technology, Kunming, 650500, China.

- 250 1. M. Sopori, *Nature Reviews Immunology*, 2002, **2**, 372-377.
- 251 2. A. Spira, J. Beane, V. Shah, G. Liu, F. Schembri, X. Yang, J. Palma and J. S. Brody, *Proceedings of*  
252 *the National Academy of Sciences of the United States of America*, 2004, **101**, 10143-10148.
- 253 3. J. M. Liddle, N. T. Mooney, G. Smith and W. C. Wright, *Journal*, 1992.
- 254 4. X. Muñoz, M.-J. Cruz, R. Orriols, C. Bravo, M. Espuga and F. Morell, *CHEST Journal*, 2003, **123**,  
255 2124-2129.
- 256 5. A. A. Fisher and A. Dooms-Goossens, *Archives of dermatology*, 1976, **112**, 1407-1409.
- 257 6. P. F. Killian, C. J. Bruell, C. Liang and M. C. Marley, *Soil & Sediment Contamination*, 2007, **16**,  
258 523-537.
- 259 7. J. Branson, J. Naber and G. Edelen, *Education, IEEE Transactions on*, 2000, **43**, 257-261.
- 260 8. T. Mensing, W. Marek, M. Raulf-Heimsoth and X. Baur, *European Respiratory Journal*, 1998,  
261 **12**, 1371-1374.
- 262 9. H.-R. Lin, *European Polymer Journal*, 2001, **37**, 1507-1510.
- 263 10. N. Wahba, M. El Asmar and M. El Sadr, *Analytical Chemistry*, 1959, **31**, 1870-1871.
- 264 11. N. Wahba, M. F. El Asmar and M. M. El Sadr, *Analytical Chemistry*, 1959, **31**, 1870-1871.
- 265 12. C. Liang, C.-F. Huang, N. Mohanty and R. M. Kurakalva, *Chemosphere*, 2008, **73**, 1540-1543.
- 266 13. K.-C. Huang, R. A. Couttenye and G. E. Hoag, *Chemosphere*, 2002, **49**, 413-420.
- 267 14. D. Amin, *Analyst*, 1981, **106**, 1217-1221.
- 268 15. M. Roushani and Z. Abdi, *Sensors and Actuators B: Chemical*, 2014, **201**, 503-510.
- 269 16. V. N. Mehta, A. K. Mungara and S. K. Kailasa, *Analytical Methods*, 2013, **5**, 1818-1822.
- 270 17. G. M. Patel, J. V. Rohit, R. K. Singhal and S. K. Kailasa, *Sensors and Actuators B: Chemical*, 2015,  
271 **206**, 684-691.
- 272 18. J. V. Rohit, J. N. Solanki and S. K. Kailasa, *Sensors and Actuators B: Chemical*, 2014, **200**,  
273 219-226.
- 274 19. J. V. Rohit and S. K. Kailasa, *Analytical Methods*, 2014, **6**, 5934-5941.
- 275 20. S. K. Laliwala, V. N. Mehta, J. V. Rohit and S. K. Kailasa, *Sensors and Actuators B: Chemical*,  
276 2014, **197**, 254-263.
- 277 21. X. Yang, J. Ling, J. Peng, Q. Cao, Z. Ding and L. Bian, *Analytica Chimica Acta*, 2013, **798**, 74-81.
- 278 22. X. Hou, S. Chen, J. Tang, Y. Xiong and Y. Long, *Analytica Chimica Acta*, 2014, **825**, 57-62.
- 279 23. C. Gao, Z. Lu, Y. Liu, Q. Zhang, M. Chi, Q. Cheng and Y. Yin, *Angewandte Chemie International*  
280 *Edition*, 2012, **51**, 5629-5633.
- 281 24. J. N. Anker, W. P. Hall, O. Lyandres, N. C. Shah, J. Zhao and R. P. Van Duyne, *Nature materials*,  
282 2008, **7**, 442-453.
- 283 25. X. Jiang, Q. Zeng and A. Yu, *Langmuir*, 2007, **23**, 2218-2223.

1			
2			
3	284	26.	L. Tang, C. Dong and J. Ren, <i>Talanta</i> , 2010, <b>81</b> , 1560-1567.
4	285	27.	R. Jin, Y. Cao, C. A. Mirkin, K. L. Kelly, G. C. Schatz and J. G. Zheng, <i>Science</i> , 2001, <b>294</b> ,
5	286		1901-1903.
6			
7	287	28.	R. Jin, Y. C. Cao, E. Hao, G. S. Métraux, G. C. Schatz and C. A. Mirkin, <i>Nature</i> , 2003, <b>425</b> ,
8	288		487-490.
9	289	29.	Q. Zhang, N. Li, J. Goebel, Z. Lu and Y. Yin, <i>Journal of the American Chemical Society</i> , 2011, <b>133</b> ,
10	290		18931-18939.
11	291	30.	G. S. Métraux and C. A. Mirkin, <i>Advanced Materials</i> , 2005, <b>17</b> , 412-415.
12	292	31.	A. Brioude and M. P. Pileni, <i>The Journal of Physical Chemistry B</i> , 2005, <b>109</b> , 23371-23377.
13	293	32.	N. Okada, Y. Hamanaka, A. Nakamura, I. Pastoriza Santos and L. M. Liz Marzán, <i>The Journal of</i>
14	294		<i>Physical Chemistry B</i> , 2004, <b>108</b> , 8751-8755.
15	295	33.	C. Xue and C. A. Mirkin, <i>Angewandte Chemie International Edition</i> , 2007, <b>46</b> , 2036-2038.
16	296	34.	Y. Chen, C. Wang, Z. Ma and Z. Su, <i>Nanotechnology</i> , 2007, <b>18</b> , 325602.
17	297	35.	M. F. de Oliveira, R. J. Mortimer and N. R. Stradiotto, <i>Microchemical Journal</i> , 2000, <b>64</b> ,
18	298		155-159.
19	299	36.	L. Zhao, S. Yang, L. Wang, C. Shi, M. Huo and Y. Li, <i>Journal of Environmental Sciences</i> , 2015, <b>31</b> ,
20	300		235-239.
21	301	37.	M. F. D. Oliveira, A. A. Saczk, J. A. G. Neto, P. S. Roldan and N. R. Stradiotto, <i>Sensors</i> , 2003, <b>3</b> ,
22	302		371-380.
23	303		
24	304		
25	305		
26	306		
27	307		
28	308		
29	309		
30			
31			
32			
33			
34			
35			
36			
37			
38			
39			
40			
41			
42			
43			
44			
45			
46			
47			
48			
49			
50			
51			
52			
53			
54			
55			
56			
57			
58			
59			
60			



**Figures**

**Fig. 1.** Characteristic absorption spectrum, TEM image and color of silver TNPs.

**Fig. 2.** UV-vis spectra of silver TNPs before and after reaction with  $(\text{NH}_4)_2\text{S}_2\text{O}_8$ .

**Fig. 3.** TEM images of silver TNPs before and after reaction with  $(\text{NH}_4)_2\text{S}_2\text{O}_8$ .

**Fig. 4.** Effects of pH on silver TNPs and  $(\text{NH}_4)_2\text{S}_2\text{O}_8$  interaction.

**Fig. 5.** Effect of reaction temperature on silver TNPs and  $(\text{NH}_4)_2\text{S}_2\text{O}_8$  interaction.

**Fig. 6.** Effect of reaction time on silver TNPs and  $(\text{NH}_4)_2\text{S}_2\text{O}_8$  interaction.

**Fig. 7.** Effect of coexistence substances.

**Fig. 8.** (A) UV-vis spectra of silver TNPs by the addition of  $(\text{NH}_4)_2\text{S}_2\text{O}_8$  concentration range from 0 to  $1.0 \text{ mmol L}^{-1}$ . (B) The linear for detection of  $(\text{NH}_4)_2\text{S}_2\text{O}_8$ .

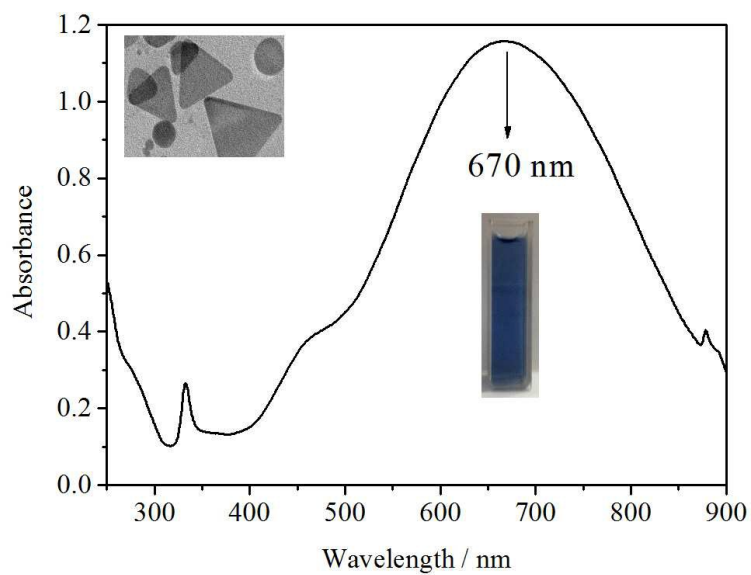


**Figure 1.** Characteristic absorption spectrum, TEM image and color of silver TNPs.

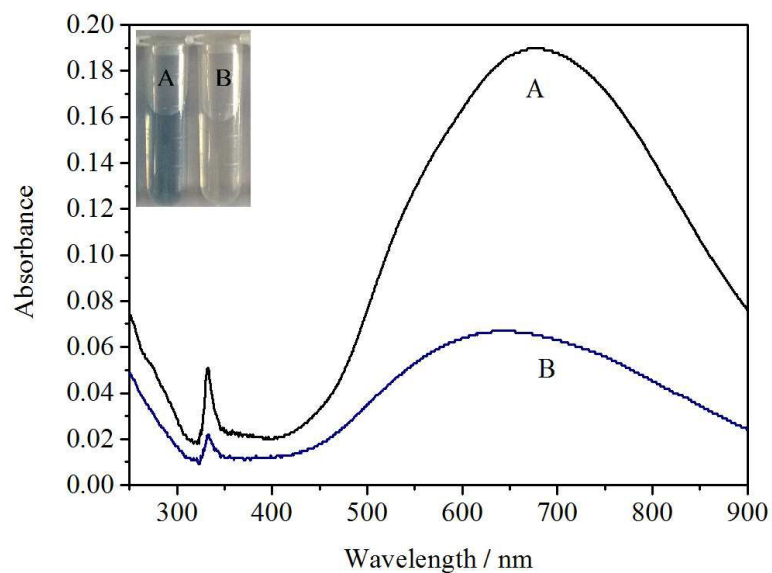


**Figure 2.** UV-vis spectra of silver TNPs before (A) and after (B) reaction with  $(\text{NH}_4)_2\text{S}_2\text{O}_8$  ( $1.0 \text{ mmol L}^{-1}$ ), pH 6.80, reaction for 30 min at  $80 \text{ }^\circ\text{C}$

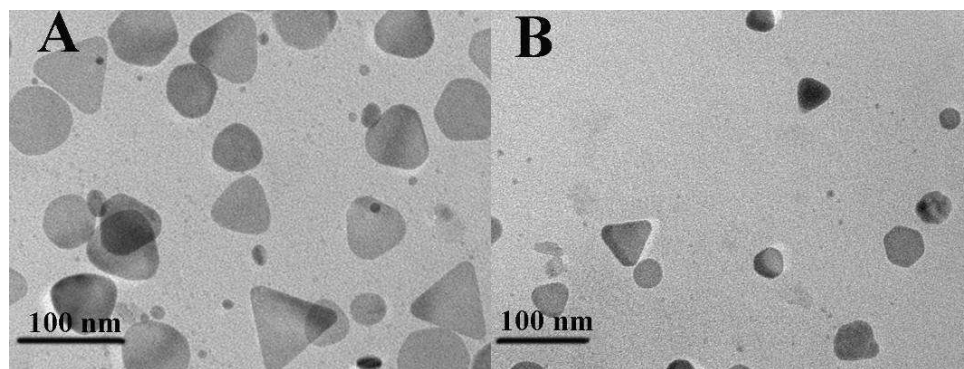


**Figure 3.** TEM images of silver TNPs before (A) and after (B) reaction with  $(\text{NH}_4)_2\text{S}_2\text{O}_8$  (0.60 mmol L<sup>-1</sup>).

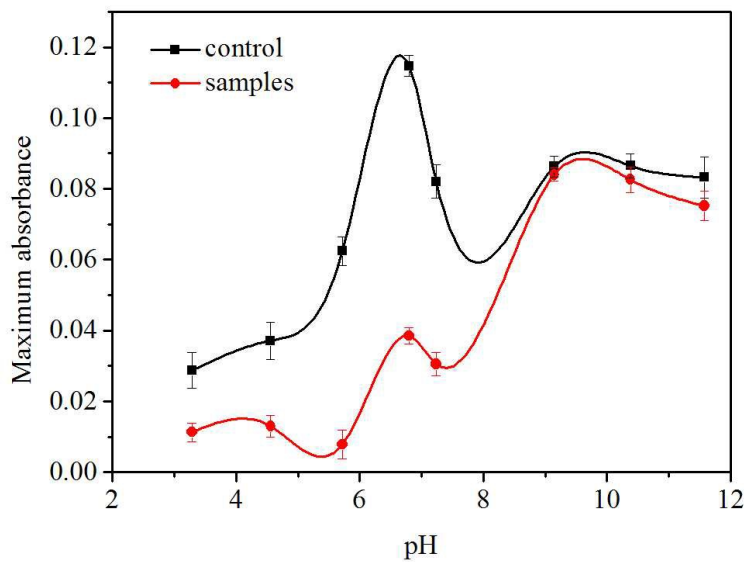


**Figure 4.** Effects of pH on silver TNPs and  $(\text{NH}_4)_2\text{S}_2\text{O}_8$  interaction. Condition: concentration of silver TNPs,  $0.286 \times 10^{-3} \text{ mol L}^{-1}$ ;  $(\text{NH}_4)_2\text{S}_2\text{O}_8$ ,  $0.60 \text{ mmol L}^{-1}$ ; B-R buffer,  $0.02 \text{ mol L}^{-1}$

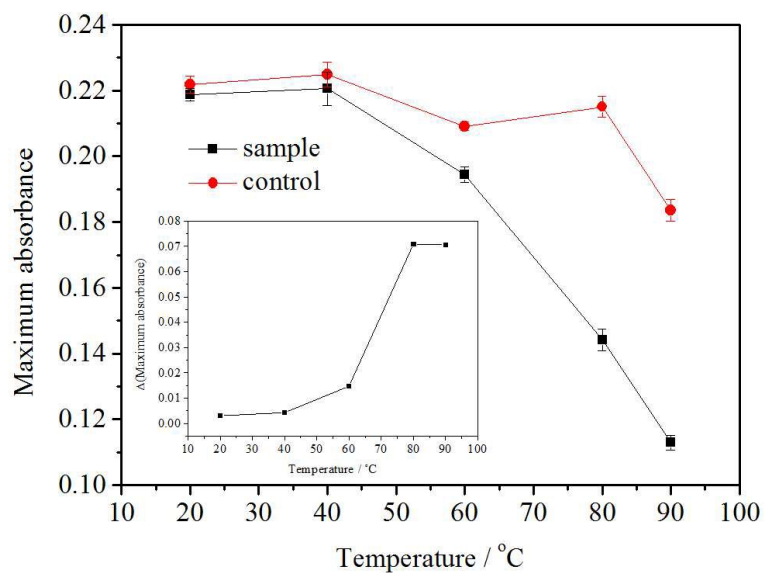


**Figure 5.** Effect of reaction temperature on silver TNPs and  $(\text{NH}_4)_2\text{S}_2\text{O}_8$  interaction.

Condition: concentration of silver TNPs,  $0.286 \times 10^{-4} \text{ mol L}^{-1}$ ;  $(\text{NH}_4)_2\text{S}_2\text{O}_8$ ,  $0.60 \text{ mmol L}^{-1}$

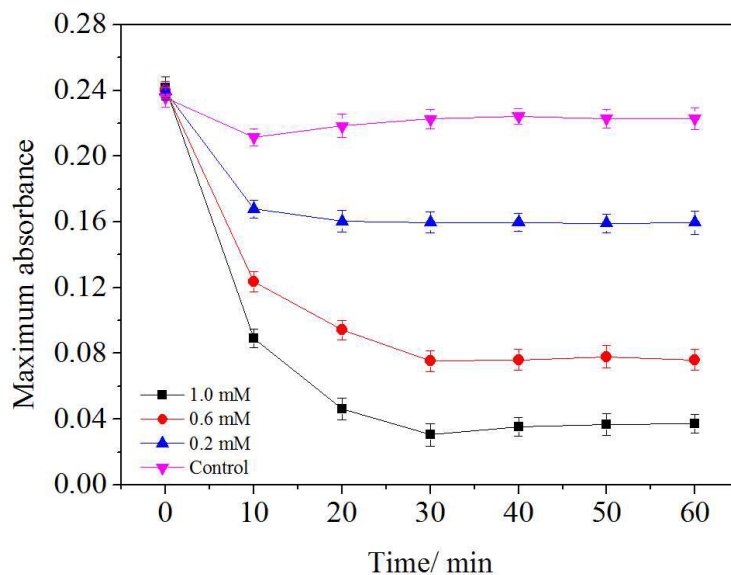


**Figure 6.** Effect of reaction time on silver TNPs and  $(\text{NH}_4)_2\text{S}_2\text{O}_8$  interaction. Four different concentrations of  $(\text{NH}_4)_2\text{S}_2\text{O}_8$  (0, 0.2, 0.6, and 1.0  $\text{mmol L}^{-1}$ ) were used for interacting with silver TNPs, concentration of silver TNPs,  $0.286 \times 10^{-3} \text{ mol L}^{-1}$

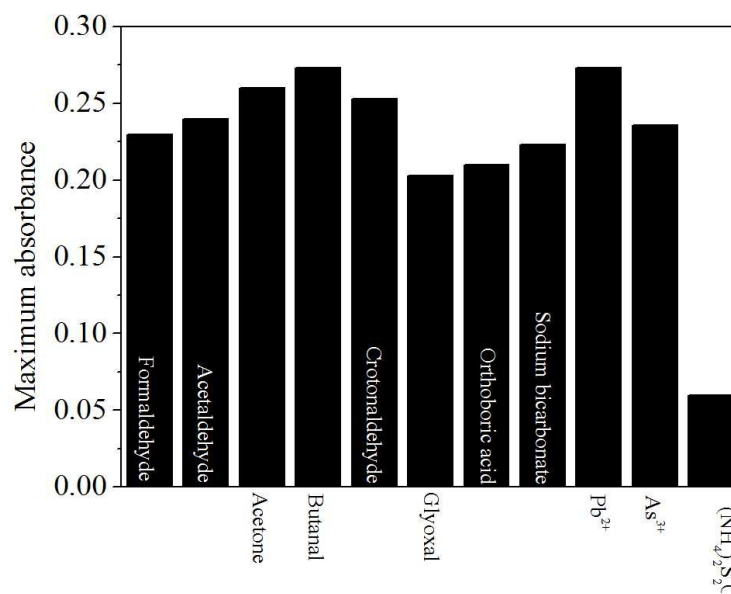


**Figure 7.** Effect of coexistence substances. Experimental condition: concentration of silver TNPs,  $0.286 \times 10^{-3} \text{ mol L}^{-1}$ ;  $(\text{NH}_4)_2\text{S}_2\text{O}_8$ ,  $0.60 \text{ mmol L}^{-1}$ ; others,  $12 \text{ mmol L}^{-1}$



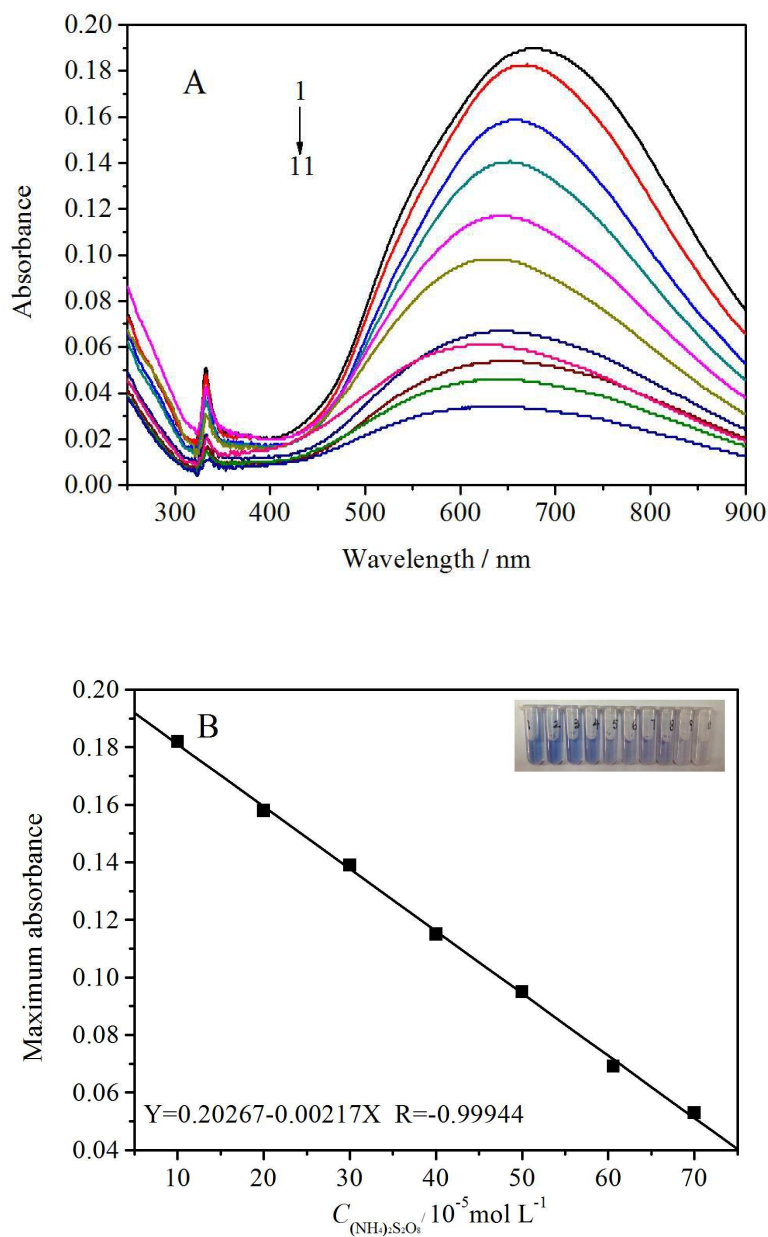


**Figure 8.** (A) UV-vis spectra of silver TNPs by the addition of  $(\text{NH}_4)_2\text{S}_2\text{O}_8$  concentration range from 0 to  $1.0 \text{ mmol L}^{-1}$  (No. 1 - 11). (B) The linear for detection of  $(\text{NH}_4)_2\text{S}_2\text{O}_8$ .